The Journal of Microbiology (2010) Vol. 48, No. 6, pp. 715-727
DOI 10.1007/s12275-010-0064-3

Assessment of Genetic and Functional Relationship of Antagonistic Fluorescent Pseudomonads of Rice Rhizosphere by Repetitive Sequence, Protein Coding Sequence and Functional Gene Analyses

Jayakumar Pathma, Niraikulam Ayyadurai, and Natarajan Sakthivel*

Department of Biotechnology, Pondicherry University, Kalapet, Puducherry 605014, India

(Received February 17, 20 / Accepted June 30, 2010)

Antagonistic fluorescent pseudomonads isolated from rice rhizospheric soil were characterized using biochemical, taxonomical and molecular tools. Production of cyclopropane fatty acid (CFA) was correlated with their antagonistic potential. Strains were grouped into 18 different genotypes on the basis of amplified ribosomal DNA restriction analysis (ARDRA) and repetitive (rep)-PCR based genotypic fingerprinting analyses. High phylogenetic resolution among antagonistic fluorescent pseudomonad strains was obtained based on the DNA gyrase B subunit (*gyrB*) and RNA polymerase sigma factor 70 (*rpoD*) gene sequence analyses. Combined *gyrB* and *rpoD* sequence analysis resulted in the accurate estimation of molecular phylogeny and provided a significant correlation between the genetic distances among strains. Present study demonstrated the genetic and functional relationship of fluorescent pseudomonads. The knowledge on genetic and functional potential of fluorescent pseudomonads associated with rice rhizosphere is useful to understand their ecological role and for their utilization in sustainable agriculture.

***Keywords*:** fluorescent pseudomonads, antagonistic potential, cyclopropane, *gyrB*, *rpoD*, rep-PCR

Rice (*Oryza sativa* L.) is the most important food crop of the world. It has been estimated that three billion people depend on rice and at least 14 countries grow rice. Fungal diseases of rice such as blast and sheath rot became production constraints in all rice-growing countries after the introduction of semi-dwarf cultivars. Chemical agents are widely used to prevent fungal diseases. Chemicals can persist and accumulate in natural ecosystems and exhibit toxicity to living organisms and also allow the development of resistance to the plant pathogens (Rainey and Moxon, 2000). Moreover, available chemical fungicides are often expensive and lethal to other beneficial rhizospheric microflora in the agricultural environment. Considering the pressing need for sustainable agriculture, biological control of fungal pathogens by antagonistic bacteria is important (Emmert and Handelsman, 1999). Antagonistic bacteria that are target-specific and eco-friendly have been used as bioinoculants and biopesticides for improving plant growth and crop yield. Among the beneficial antagonistic microbial population, fluorescent pseudomonads have been reported as the most predominant bacteria in plant rhizosphere (Kumar and Dube, 1992). Knowledge on genetic structure and functional diversity of antagonistic fluorescent pseudomonads is essential for their applications as well as for understanding their ecological role in sustainable agriculture (Rangarajan *et al*., 2001). In our earlier studies, we have reported specific fluorescent pseudomonad strains that exhibit plant growth promoting traits, production of antibiotics and biodegradation potential (Ayyadurai *et al*., 2006, 2007; Ravindra and Sakthivel, 2006).

* For correspondence. E-mail: puns2005@gmail.com; Tel: +91-413-265-4430, -5715; Fax: +91-413-265-5255

Cyclopropane fatty acids (CFA) are major component of the phospholipids of many species of bacteria (Grogan and Cronan, 1997). These acids are formed by addition of a methylene group, derived from the methyl group of S-adenosyl methionine, across the carbon-carbon double bond of unsaturated fatty acids (UFAs) (Grogan and Cronan, 1997). Microbial cells having high levels of CFA survived during acid shock much more efficiently than those strains with low CFA levels. CFA showed a strong correlation between the resistances towards various environmental factors (Brown *et al*., 1997) and could be one of the factor which influences accurate functioning in a rapidly changing environment. It has been proved that the CFA plays an important role in adaptation processes in the unstable pH. Earlier study has confirmed the correlation of CFA towards the antagonistic potential of fluorescent pseudomonad strains (Ayyadurai *et al*., 2007). The present report describes the characterization of these antagonistic strains of fluorescent pseudomonads, their functional potential and genetic relationships by genomic fingerprinting analyses and combined *gyrB* and *rpoD* DNA sequence analyses.

Materials and Methods

Microbial cultures

Reference strains, *Pseudomonas fluorescens* Pf-5, *P. fluorescens* 2-79, *P. aeruginosa* PAO1 were kindly supplied by Linda S. Thomashow, USDA, Washington State University, Pullman, USA, *P. fluorescens* CHAO was obtained from Genevieve Defago, Institute of Plant Sciences, Swiss Federal Institute of Technology, Zurich, Switzerland and *P. stutzeri* MTCC 863 was obtained from the Microbial Type Culture Collection (MTCC), Chandigarh. Microbial cultures were maintained at the Department of Biotechnology, Pondicherry University, Pondicherry.

Isolation and screening of antagonistic fluorescent pseudomonads

Fluorescent pseudomonads were isolated from rhizospheric samples of rice as described (Sakthivel and Gnanamanickam, 1987). Single colonies were selected and further cultured onto King's B agar (KBA) (King *et al*., 1954) to establish pure cultures. Bacteria were tested for *in vitro* antagonism towards fungal pathogens, *Rhizoctonia solani* (sheath blight of rice), *Magnoporthe grisea* (rice blast), *Sarocladium oryzae* (sheath rot), *Macrophomina phaseolina* (charcoal rot of groundnut), *Fusarium oxysporum* f. sp. *vasinfectum* (wilt of cotton), *Pestalotia theae* (leaf spot of tea), *Colletotrichum capsici* (fruit rot of chili), *C. falcatum* (red rot of sugarcane), *C. gleosporoides* (anthracnose of mango), *Cylindrocladium floridanum* (root necrosis of banana), *Cy. scoparium* (root necrosis of banana) by standard co-inoculation technique on potato dextrose agar (PDA) (Sakthivel and Gnanamanickam, 1987).

Culture dependent biochemical characterization

Biochemical tests such as fluorescence on KB agar, arginine dihydrolase, oxidase, gelatin hydrolysis, levan production and growth at 4°C and 42°C were performed as described (Bossis *et al*., 2000). Substrate utilization profiles were tested using Hicarbohydrate™ kits (Himedia Laboratories, Mumbai, India) as per the manufacture protocol. Data was converted to the binary code and distance matrix was calculated by using pairwise co-efficient of similarity (Dice). Cluster analysis was done by using the unweighted pair group method with average (UPGMA) algorithm of NTSYSpc2 (Version 2.02a, Exeter software, USA) numerical taxonomy and multivariate analysis system.

Fatty acid methyl ester analyses (FAME)

Bacterial strains were grown on tryptic soy agar (TSA) in triplicate and incubated at 28°C for 24 h. Cells (50 mg wet weight) were scraped and suspended in 1 ml of saponification reagent in a screw cap test tube and vortexed for 10 sec. The tube was then placed in the water bath at 100°C for 25 min, cooled to room temperature, and 2 ml of methylation reagent was added. The mixture was then vortexed for 10 sec, placed in a water bath at 80°C for 10 min and rapidly cooled by placing on ice. Then, extraction buffer (1.25 ml) was added and mixed well for 10 min. The aqueous lower layer was separated and discarded. To the upper organic phase, 3 ml of base wash reagent was added and mixed well for 5 min. The mixture was then centrifuged at 3,000 rpm for 5 min. The upper solvent phase was removed and analyzed by gas-liquid chromatography (Hewlett-Packard 6890, USA) using capillary column Ultra 2-HP (cross-linked 5% phenyl-methyl silicone; 25 m, 0.22 mm, film thickness; 0.33 μm) and hydrogen as the carrier gas. FAME compounds were detected by a flame ionization detector (FID) and identified using the Microbial Identification Software (Sherlock aerobe method and TSBA40 Library Version 4.5) developed by MIDI Inc., Newark, DE, USA. Non-antagonistic fluorescent pseudomonad strains were used as control. Reference strain *P. fluorescens* 2-79 was used as positive control.

Determination of plant growth promoting rhizobacterial (PGPR) traits

Siderophore

Production of siderophore was determined using chrome azurol S agar (CAS) assay. Briefly, inoculum (10 μl) was dropped onto the center of a CAS plate. After incubation at 28°C for 5 days, siderophore production was assessed by change in the color of the medium from blue to orange (Schwyn and Neiland, 1987).

Indole-3-acetic acid (IAA)

The production of IAA was determined using standard method (Bric *et al*., 1991). Single colony was streaked onto Luria-Bertani (LB) agar amended with 5 mM L-tryptophan, 0.06% sodium dodecyl sulphate (SDS), and 1% glycerol. Plates were overlaid with sterile Whatman no. 1 filter paper (82 mm diameter) and the bacterial strain was allowed to grow for 3 days at 28°C. After the incubation period, the paper was removed and treated with Salkowski's reagent (Gordon and Weber, 1951) having a formulation of 2% of 0.5 M ferric chloride in 35% perchloric acid at room temperature for 60 min. In a petri dish, the filter papers were saturated by soaking in Salkowski's reagent and the production of IAA was identified by the formation of a characteristic red halo on the paper immediately surrounding the colony. For quantification of IAA, bacterial strains were grown on Luria-Bertani (LB) broth amended with 5 mM L-tryptophan, 0.06% sodium dodecyl sulphate (SDS) and 1% glycerol and IAA produced was determined (Patten and Glick, 2002) using the colorimetric method described earlier (Gordon and Weber, 1951).

Aminocyclopropane-1-carboxylate (ACC) deaminase

The ACC deaminase activity was determined by using DF salts medium, which contains (per L): 4.0 g KH_2PO_4, 6.0 g Na_2HPO_4, 0.2 g $MgSO_4 \cdot 7H_2O$, 2.0 g $(NH_4)_2SO_4$, 2.0 g gluconic acid and 2.0 mg citric acid with trace element solution (1.0 mg $FeSO_4 \cdot 7H_2O$, 10 μg H_3BO_3, 11.19 μg $MnSO_4 \cdot H_2O$, 124.6 μg $ZnSO_4 \cdot 7H_2O$, 78.22 μg $CuSO_4 \cdot 5H_2O$, and 10 μg MoO_3). Filter sterilized ACC solution (3.0 mM) was spread over the agar plates, allowed to dry for 10 min, and inoculated with bacterial strains. Observation of the growth was made after 2 days of incubation at 28°C as described (Penrose and Glick, 2002).

Phosphatase

To determine the production of phosphatase, bacterial strains were streaked onto Pikovskaya's agar, which contains (per L): 0.5 g yeast extract, 10 g dextrose, 5.0 g $Ca_3(PO_4)_2$, 0.5 g $(NH_4)_2SO_4$, 0.2 g KCl, 0.1 g $MgSO_4 \cdot 7H_2O$, 0.0001 g $MnSO_4 \cdot H_2O$, 0.0001 g $FeSO_4 \cdot 7H_2O$, and 15 g agar. After 3 days of incubation at 28°C, strains that induced clear zone around the colonies were considered as positive (Ravindra *et al*., 2008). Determination of phosphate solubilizing activity by the strains was carried out following standard method (King, 1936). Briefly, bacterial strains were grown in Pikovskaya's broth (pH 7.0) at 28°C upto 10 days. A 5 ml aliquot was collected after 1, 3, 5, 7 and 10 days and the cells were removed by centrifugation at 9,000×g for 20 min. Soluble free phosphate in culture supernatant was estimated from the absorbance values obtained using the calibration curve with KH_2PO_4 at 600 nm for each strain. Also, pH variation in Pikovskaya's broth during the growth of each strain was also observed.

Denitrification activity

To determine the denitrification activity, nitrate reduction test was carried out. Bacterial strains were grown in 5 ml of nitrate medium (Dye, 1962) which contains (per L): 2.0 g KNO3, 10 g peptone and 5.0 g NaCl. At intervals upto 5 days an aliquot of 1 ml culture was withdrawn and tested for nitrite formation by adding a few drops of sulphanilic acid (0.8 g of sulphanilic acid dissolved in 100 ml of 5 N acetic acid) and α-naphthylamine reagent (0.5 g of α-napthylamine dissolved in 100 ml of 5 N acetic acid). A distinct pink or red colour indicated the presence of nitrite.

Detection of denitrification and antibiotic genes

Bacterial strains were grown in LB broth at 28°C for 18 h. Total

genomic DNA was extracted as described (Leach *et al*., 1992). DNA pellets were resuspended in 40 µl of TE buffer (10 mM Tris-HCl, 1 mM EDTA; pH 8.0) and treated with RNase at 37°C for 30 min. Purity and the concentration of DNA were estimated in a U2000 spectrophotometer (Hitachi Ltd., Japan). Oligonucleotide primers were synthesized by Integrated DNA Technologies Inc. (USA). Gene-specific primers were used to detect the genes encoding nitrate reductase (*narG*) and nitrous oxide reductase (*nosZ*), that catalyze the first and last steps of denitrification, respectively. PCR conditions were used as described (Delorme *et al*., 2003). Reference strain *P. stutzeri* MTCC 863 was used as control. Detection of the genes that encode antibiotics such as, 2,4-diacetylphloroglucinol (DAPG), phenazine-1-carboxylic acid (PCA), phenazine-1-carboxamide (PCN), pyrrolnitrin (PRN), and pyoluteorin (PLT) was done by PCR using gene-specific primers as described (Ravindra *et al*., 2008). Reference strains, *P. fluorescens* Pf5, *P. fluorescens* 2-79, *P. aureofaciens* 30-84 (now considered as *P. chlororaphis*), and *P. aeruginosa* PAO1 were used as control. Primer sequences and amplification conditions are presented in Table 1. PCR reaction (50 µl) contained 50 pM of each primer, 50 ng of genomic DNA, 1× *Taq* DNA polymerase buffer, 1 U of *Taq* DNA polymerase (Promega, USA), 0.2 mM of each dNTP, and 1.5 mM $MgCl_2$. Amplification was performed in a DNA thermal cycler (2400 cycler, Perkin Elmer International, Rotkreuz, Switzerland). A 5 µl aliquot of each amplified product was electrophoresed on a 0.7% agarose gel in 1× tris acetate ethylenediaminetetraacetic acid (TAE) buffer at 50 V for 45 min, stained with ethidium bromide and the PCR products were visualized under UV transilluminator.

Production of antifungal compounds

Putative strains were further verified for antibiotic production using analytical high-performance liquid chromatography (HPLC). Briefly, purified extracts were resuspended in 1 ml of methanol (HPLC grade) and subjected to C_{18} reverse-phase HPLC (Phenomenex Luna, 250×10 mm) with 30 µl injection volumes. The solvent conditions included a flow rate of 0.7 ml/min with acetonitrile and water (both containing 0.1% trifluroacetic acid) in a 30 to 70% linear gradient for PCA (Thomashow *et al*., 1990). The solvent conditions included a flow rate of 2 ml/min with 80% acetonitrile in water for DAPG (Keel *et al*., 1992). HPLC gradient profiles were monitored at 257 nm for PCA, 270 nm for DAPG, 220 nm for PRN and 255 nm for PLT using UV detector 10 AVP (Shimadzu, Japan). Authentic standard samples were used as controls. Production of antibiotics by the strains was confirmed by specific retention time as described earlier (Sunish *et al*., 2005; Ravindra *et al*., 2008). Thin Layer Chromatography (TLC) was carried out on silica gel G60 (20×20 cm; 0.25 mm thick; Selecto Scientific, USA). The plates were activated at 110°C for 30 min, cooled, spotted with ethanol solution containing standard antibiotics (0.5 µg) and 20 µl of extract. Separation was performed with chloroform-methanol (9:1 v/v) for PCA and DAPG or chloroform-acetone (9:1 v/v) for PLT and PRN. The corresponding spots by PCA, DAPG were detected by ultraviolet (UV) at 254 nm (Thomashow *et al*., 1990). PLT spots were detected by spraying with an aqueous 0.5% Fast Blue RR salt solution and the PRN spots were detected by spraying the TLC plates with 2% p-dimethylaminobenzaldehyde (Ehrlich reagent) dissolved in the ethanol-sulfuric acid (1:1 v/v) (de Souza and Raaijimakers, 2003).

Amplification of *gyrB* and *rpoD* genes and molecular phylogeny analysis

The *gyrB* and *rpoD* genes were amplified as described by Yamamoto *et al*. (2000). The primer pairs, *GYRB*F and *GYRB*R for *gyrB* and *RPOD*F and *RPOD*R for *rpoD* were used. Primer sequences and

Table 1. Primers and amplification conditions used in the study

Primer set	Primer	Sequence (5′→3′)	References	Amplification conditions
16S	fD1 rP2	5′-GAGTTTGATCCTGGCTCA-3′ 5′-ACGGCTACCTTGTTACGACTT-3′	Weisburg *et al*. (1991)	Initial denaturation at 94°C for 1 min, 30 cycles, 94°C for 1 min, 46°C for 30 sec and 72°C for 30 sec. Final extension at 72°C for 5 min.
gyrB	GYRBF GYRBR	5′-CAGGAAACAGCTATGACCAYG 5′-TGTAAAACGACGGCCAGTGCN GGRTCYTTYTCYTGRCA-3′	Yamamoto *et al*. (2000)	Initial denaturation 94°C for 3 min, 30 cycles, 2 min. Final extension at 72°C of 5 min
rpoD	RPODF RPODR	5′-ACGACTGACCCGGTACGCATG TAYATGMGNGARATGGGNACNGT-3′ 5′-ATAGAAATAACCAGACGTAAGTT NGCYTCNACCATYTCYTTYTT-3′	Yamamoto *et al*. (2000)	Initial denaturation 94°C for 3 min, 30 cycles, 94°C for 1 min, 59°C for 1 min and 72°C for 2 min. Final extension at 72°C 5 min.
ERIC	ERIC-1R ERIC-2	5′-ATGTAAGCTCCTGGGGATTCAC-3′ 5′-AAG TAAGTGACTGGGGTGAGCG-3′	Bhattacharya *et al*. (2003)	Initial denaturation 95°C for 7 min, 30 cycles of 94°C for 1 min, 52°C for 1 min, and 65°C for 8 min. Final extension at 65°C for 15 min.
REP	REP 1R DT REP 2-DT	5′-IIIICGICGICATCIGGC-3′ 5′-ICGICTTATCIGGGCTAC-3′	-do-	Initial denaturation 95°C for 7 min, 30 cycles of 94°C for 1 min, 44°C for 1 min, and 65°C for 8 min. Final extension at 65°C for 15 min.
BOX	BOXAIR	5′-CTACGGCAAGGCGACGCTGACG-3′	-do-	Initial denaturation 95°C for 7 min, 30 cycles of 94°C for 1 min, 53°C for 1 min, and 65°C for 8 min. Final extension at 65°C for 15 min.
narG	narGf narGr	5′-GA[C/T]ATGCA [C/T]CC[A/C/G/T]TT-3′ 5′-A[C/T]CCA[A/G]TC[A/G]TT[A/G]TC-3′	Delorme *et al*. (2003)	Initial denaturation 94°C for 3 min, 30 cycles of 94°C for 1 min, 54°C for 1 min, and 72°C for 1 min. Final extension at 72°C for 3 min.
nosZ	nosZf nosZr	5′-AACGACAAG[G/A/T][C/T]CAA-3′ 5′-A[G/T][G/C]GC [A/G]TGGCAGAA-3′	Delorme *et al*. (2003)	Initial denaturation 94°C for 3 min, 30 cycles of 94°C for 1 min,62°C for 1 min, and 72°C for 2 min. Final extension at 72°C for 3 min.

Table 2. Functional traits of antagonistic fluorescent *Pseudomonas* of rice

Strain	Closest hits to sequences in NCBI database	Sequence homology (%)	GenBank accession no.		Plant growth promoting rhizobacterial traits and antibiotics									
			gyrB	*rpoD*	IAA	PS	ACC	*narG*	*nosZ*	DAPG	PCA	PCN	PRN	PLT
P1	*Pseudomonas pseudoalcaligenes*	97	DQ201342	DQ201367	–	–	–	–	–	–	–	–	–	–
P2	*Pseudomonas fluorescens*	89	DQ201343	DQ201368	–	+	–	+	–	+	–	–	+	+
P3	*Pseudomonas fluorescens*	99	DQ201344	DQ201369	–	+	–	+	–	+	–	–	+	+
P4	*Pseudomonas pseudoalcaligenes*	98	DQ201345	DQ201370	–	–	+	+	–	–	–	–	–	–
P5	*Pseudomonas fluorescens*	97	DQ201346	DQ201371	–	+	–	–	–	+	–	–	–	+
P6	*Stenotrophomonas maltophilia*	99	DQ201347	DQ201372	–	+	–	+	–	–	–	–	–	–
P7	*Pseudomonas fluorescens*	97	DQ201348	DQ201373	–	+	–	–	–	+	–	–	+	+
P8	*Pseudomonas fluorescens*	96	DQ201349	DQ201374	–	–	–	+	–	+	–	–	+	+
P9	*Pseudomonas fluorescens*	96	DQ201350	DQ201375	–	+	–	–	–	–	–	–	–	+
P10	*Pseudomonas aeruginosa*	99	DQ201351	DQ201376	+	+	–	–	–	+	–	–	–	–
P11	*Pseudomonas aeruginosa*	93	DQ201352	DQ201377	+	+	–	–	–	–	–	–	–	–
P12	*Pseudomonas putida*	92	DQ201353	DQ201378	+	+	–	–	–	–	–	–	–	–
P13	*Pseudomonas aeruginosa*	99	DQ201354	DQ201379	+	+	–	+	+	–	–	–	–	–
P14	*Pseudomonas fluorescens*	99	DQ201355	DQ201380	–	+	–	–	–	+	–	–	+	+
P15	*Pseudomonas putida*	99	DQ201356	DQ201381	–	+	–	+	–	–	+	–	+	–
P16	*Pseudomonas fluorescens*	99	DQ201357	DQ201382	–	+	–	+	–	–	–	–	–	–
P17	*Pseudomonas fluorescens*	99	DQ201358	DQ201383	–	+	–	+	–	–	–	–	–	–
P18	*Pseudomonas fluorescens*	92	DQ201359	DQ201384	–	–	–	–	–	+	–	–	+	+
P19	*Pseudomonas fluorescens*	98	DQ201360	DQ201385	–	–	–	+	–	–	–	–	+	+
P20	*Pseudomonas plecoglossicida*	98	DQ201361	DQ201386	–	–	–	+	–	–	–	–	–	–
P21	*Pseudomonas fluorescens*	98	DQ201362	DQ201387	–	–	–	–	–	+	–	–	+	+
P22	*Pseudomonas fluorescens*	96	DQ201363	DQ201388	–	–	–	–	–	–	–	–	+	+
P23	*Pseudomonas fluorescens*	99	DQ201364	DQ201389	–	+	–	+	–	–	–	–	–	–
P24	*Pseudomonas putida*	98	DQ201365	DQ201390	–	+	+	–	–	–	–	–	–	–
P25	*Pseudomonas putida*	98	DQ201366	DQ201391	–	+	–	–	–	–	–	–	–	–

IAA, indole-3-acetic acid; PS, phosphate solubilization; ACC, 1-aminocyclopropane-1-carboxylate deaminase; *narG*, nitrate reductase; *nosZ*, nitrous oxide reductase; DAPG, 2,4-diacetylphloroglucinol; PCA, phenazine-1-carboxylic acid; PCN, phenazine-1-carboxamide; PRN, pyrrolnitrin; PLT, pyoluteorin. The nucleotide-nucleotide BLAST search tool (BLASTN) of the National Center for Biological Information (NCBI, USA) was used to find closest hits (sequences) in the relevant databases that better match to our queries.

amplification conditions are presented in Table 1. The reference sequences required for comparison were obtained from the National Centre for Biotechnology Information (NCBI) database using the site http://www.ncbi.nlm.nih.gov/Genbank. All the sequences of *gyrB* and *rpoD* of antagonistic fluorescent pseudomonad strains were aligned using the multiple sequence alignment program CLUSTAL V (Higgins *et al*., 1992). The aligned sequences were then checked for gaps manually, arranged in a block of 250 bp in each row and saved as molecular evolutionary genetics analysis (MEGA) format in software MEGA v2.1. The pair wise evolutionary distances were computed using the Kimura 2-parameter model (Kimura, 1980). To obtain the confidence values the original data set was resampled 1,000 times using the bootstrap analysis method. The bootstrapped data set was used directly for constructing the phylogenetic tree using the MEGA program or used for calculating the multiple distance matrixes. The multiple distance matrix obtained was then used to construct phylogenetic trees using neighbor-joining (NJ) method of Saitou and Nei (1987). The correlations between the distances in the *gyrB* and *rpoD* genes were obtained by the method of Nei and Gojobori (1986). All these analysis were performed using the MEGA v 2.1 (Kumar *et al*., 2001). Phylogenetic tree was also reconstructed from the data sets of *gyrB* and *rpoD*, as well as from the combined nucleotide sequences of these two genes from the same strain to achieve better resolution and reliability.

Amplified ribosomal DNA restriction analysis (ARDRA)

Amplification of ribosomal DNA (16S rRNA) was performed from the genomic DNA templates of antagonistic bacteria as described earlier, using universal primers, fD1 and rP2 (Weisburg *et al*., 1991). Primer sequences and amplification conditions are presented in Table 1. The 16S rRNA fragments were digested with 11 different restriction enzymes (*Alu*I, *Bam*HI, *Pvu*II, *Hind*III, *Hae*III, *Hha*I, *Nhe*I, *Sph*I, *Pst*I, *Kpn*I, and *Taq*I) at 37°C for 2 h. The digested products were electrophoresed on a 12% native acrylamide gel and stained with ethidium bromide. A combined dendrogram was constructed using the BIO-GENE software program (Version 11.02; Vilber Lourmat, France). Cluster analysis of similarity matrices was performed by the UPGMA algorithm by Dice coefficient.

Repetitive (rep)-PCR based genotypic fingerprinting [repetitive extragenic palindromic (REP) elements, enterobacterial repetitive intergenic consensus (ERIC) and BOX analysis]

Primer sequences and amplification conditions for rep-PCR are presented in Table 1. A 10 µl of PCR product was separated using 1.5% agarose gel stained with ethidium bromide in 1× TAE. The image of the gel was digitized by using BIO-CAPT system (Vilber Lourmat, France) and stored as TIFF files. Computer-assisted analysis of genomic fingerprints was performed by using the BIO-GENE software program (Version 11.02; Vilber Lourmat, France). Similarity matrices of whole densitometric curves of the gel tracks were calculated by using the Dice coefficient. Cluster analysis of similarity matrices was performed by the UPGMA algorithm.

Synonymous and non-synonymous substitutions analysis

The relative rates of synonymous and non-synonymous substitutions are good indicators of the amount and type of selection affecting a gene (Sharp, 1997). We have estimated the synonymous substitutions per synonymous site (dS) and non-synonymous substitutions per non-synonymous site (dN) by using the method of Nei and Gojobori (1986) in the MBE Tool box package under MAT lab platform (Cai *et al*., 2005). These methods perform pair wise comparisons of sequences from protein coding genes and compare the results with those of the likelihood analysis assuming different models.

Nucleotide sequence accession numbers

The GenBank accession no. of the *gyrB* and *rpoD* nucleotide sequences of the strains deposited in NCBI and are presented in Table 2.

Results

Isolation and screening of antagonistic fluorescent pseudomonads

Of 750 fluorescent pseudomonad strains isolated from rice rhizosphere, 25 strains showed growth inhibitory activity towards phytopathogenic fungi. Strains showed varying degree of antifungal activity by inducing mycelial growth inhibition zones (diameter) ranging from 3 to 35 mm. While strains P10, P11, P12, P13, P24, and P25 showed broad-spectrum activity against all fungal pathogens tested in this study other antagonistic strains exhibited activity against more than one fungal pathogen (Table 3).

Table 3. Antifungal activity of fluorescent pseudomonads

Fungus	Disease	Host	Antagonistic strains
Rhizoctonia solani RSR1	Sheath blight	Rice	P2, P3, P4, P7, P10, P11, P12, P13, P24, P25
Magnoporthe grisea MGS	Blast	Rice	P1, P2, P3, P4, P5, P6, P7, P8, P10, P11, P12, P13, P17, P19, P21, P23, P24, P25
Sarocladium oryzae SONS	Sheath rot	Rice	P2, P4, P6, P7, P9, P10, P11, P12, P13, P15, P16, P17, P19, P20, P21, P22, P24, P25
Macrophomina phaseolina MPS	Charcoal rot	Groundnut	P1, P7, P10, P11, P12, P13, P14, P15, P16, P17, P18, P19, P21, P22, P23, P24, P25
Fusarium oxysporum f. sp *vasinfectum* FOVS	Wilt	Cotton	P7, P10, P11, P12, P13, P24, P25
Pestalotia theae PTS	Leaf spot	Tea	P2, P3, P7, P10, P11, P12, 13, P15, P17, P19, P22, P24, P25
Colletotrichum capsici CCL	Fruit rot	Chili	P7, P10, P11, P12, P13, P15, P16, P17, P19, P21, P24, P25
C. falcatum CFL	Red rot	Sugarcane	P7, P10, P11, P12, P13, P14, P15, P20, P21, P24, P25
C. gleosporoides CGL	Anthracnose	Mango	P7, P10, P11, P12, P13, P14, P15, P20, P21, P24, P25
Cylindrocladium floridanum ATCC 42971	Root necrosis	Banana	P10, P11, P12, P13, P24, P25
Cy. scoparium ATCC 46300	Root necrosis	Banana	P10, P11, P12, P13, P24, P25

Culture dependent analysis of functionally associated fluorescent pseudomonads

All the strains tested positive for fluorescence on KB, oxidase and arginine dihydrolase. However, strains also showed variation in the traits such as gelatin hydrolysis, levan production and growth at 4°C and 42°C. Although, these tests are considered to be important for discrimination among species of fluorescent pseudomonads, in our study the specific characters did not contribute for the discrimination among the antagonistic fluorescent pseudomonads. On the other hand, all the tests showed phenotypic diversity among the antagonistic fluorescent pseudomonads. All strains utilized dextrose, galactose, mannose and citrate but exhibited varying degree of utilization profile towards other carbon sources such as lactose, xylose, fructose, melibiose, L-arabinose, glycerol, ribose, methyl-D-mannoside, xylitol, esculin, D-arabinose, malonate, sorbose, trehalose, sorbitol, mannitol, adonitol, and glucosamine but did not utilize maltose, sucrose, inulin, salicin, dulcitol, inositol, α-methyl-D-gluconate, rhamnose, cellobiose, xylitol, and ONPG. Based on these phenotypic traits, 11 strains were grouped as *P. fluorescens*, 7 strains as *P. putida,* 3 isolates as *P. aeruginosa*, 3 strains as *P. chlororaphis* and 1 strain as an intermediate between *P. fluorescens* and *P. putida*. Among antagonistic strains, 7 strains that did not liquefy gelatin were identified as *P. putida*, while 11 strains that hydrolysed alanine were identified as *P. fluorescens*. The remaining strains that did not hydrolyse alanine were identified as *P. aeruginosa*. Based on the phenotypic characterization, majority of the antagonistic fluorescent pseudomonads were identified as *P. fluorescens*. We have also differentiated the *P. fluorescens* and *P. putida* biovars due to their ability to utilize different carbon sources. Based on this observation, a total of 11 strains were identified as *P. fluorescens* biovar III, 3 strains as *P. fluorescens* biovar V and one strain as *P. fluorescens* biovar II. On the other hand, 6 strains were identified as *P. putida* biovar B and one strain as *P. putida* biovar A. Numerical analysis of phenotypic characteristics revealed a high degree of polymorphism. Strains were grouped into 3 different phenons on the basis of phenotypic traits (Fig. 1). The similarity range among antagonistic strains was 0.65 to 0.94. The first phenon consisted of the majority of the antagonistic strain (14 strains) such as P1-P3, P8, P12, P14, P15, P17-P23 and shared approximately 0.76 similarity index, second phenon consisted of 7 strains (P4, P5, P10, P11, P13, P24, and P25) with 0.70 similarity index. The third phenon contained only three *P. fluorescens* strains (P7, P9, P16) with 0.74 similarity index. These results suggested that phenotypic characters could be useful in identification of strains at the genus level and not stable at the species level.

Fatty acid methyl ester analysis

Under standardized growth conditions all strains displayed qualitatively similar FAME profiles. In FAME analysis, the proportion of fatty acid in each antagonistic strain was identified as a variable. Characteristic presence of high relative proportions (0.7% to 14%) of cyclopropane fatty acid (CFA) (17:0 CYCLO w7c) was observed in all antagonistic fluorescent pseudomonad strains. The reference strain, *P. fluorescens* 2-79 showed 4.1% of CFA. FAME analysis did not show detectable level of CFA in non-antagonistic control strains.

Functional characterization of antagonistic fluorescent pseudomonads

Functional characterization of fluorescent pseudomonads revealed a considerable variation in the production of metabolites and enzymes. While all strains were able to produce siderophores, a total of 17 strains exhibited phosphate solubilizing activity, 4 strains exhibited IAA production, 12 strains showed denitrification activity and 2 strains tested

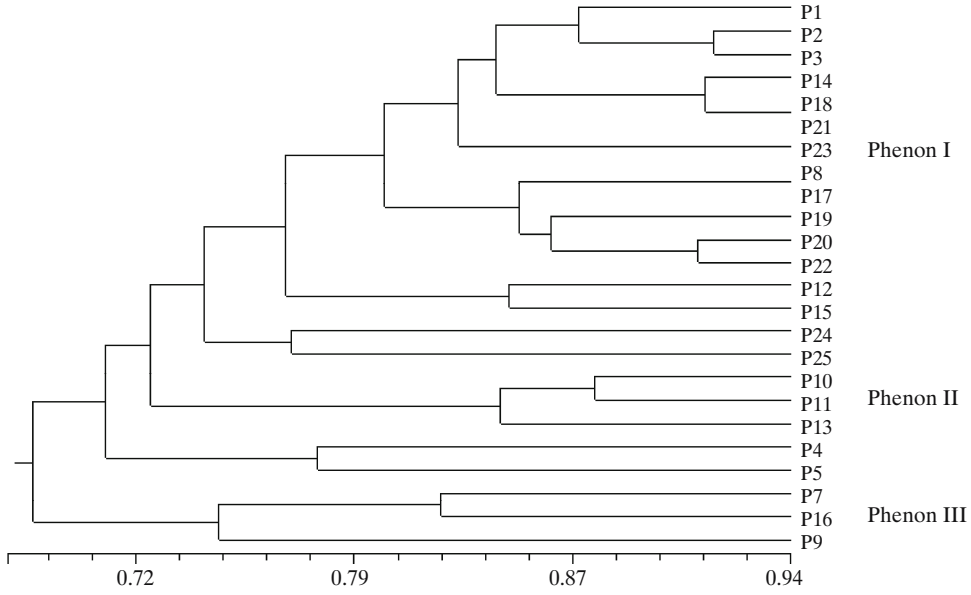

Fig. 1. Dendrogram of antagonistic fluorescent pseudomonads based on their phenotypic traits. The pairwise coefficients of similarity (Dice) were clustered with the UPGMA algorithm of NTSYS-pc2. The antagonistic strains were grouped into 3 phenons.

positive for ACC deaminase activity (Table 2). The IAA positive strains, P10, P11, P12, and P13 produced 25.5, 25, 9.5, and 43 µg/ml of IAA respectively. Phosphate solubilization initiated on day1 and it reached the maximum on 10 days after incubation for all strains (Table 4).

Detection of denitrification and antibiotic genes and production of antifungal compounds

Primers *narG* and *nosZ* amplified the DNA fragment of about 1,008 bp and 1,433 bp, respectively. The reference strain *P. stutzeri* MTCC 863 showed positive amplification for both *narG* and *nosZ* gene. Among the antagonistic strains, only strain P13 showed positive amplification for both *narG* and *nosZ* and 12 strains showed positive amplification for *narG*. When templates of antagonistic strains were tested with gene-specific primers of PCA, DAPG, PLT, PRN, and PCN, 9 strains amplified the DNA fragment of 745-bp of DAPG, 10 strains amplified the DNA fragment of 719-bp of PRN, 11 strains amplified DNA fragment of 779-bp of PLT and one strain amplified DNA fragment of 1,100-bp of PCA (C, D) (Table 2). Results revealed that a total of 11 strains showed the presence of more than one antibiotic genes and 12 strains did not show the amplification of any known antibiotic genes (Table 2). HPLC analyses confirmed the production of antibiotics by the putative strains. The antifungal metabolites such as DAPG (yellowish white), PCA (greenish yellow), PRN (light yellow), and PLT (yellowish white) were extracted from the fermentation cultures of PCR positive strains. The production of antibiotics by antagonistic strains was confirmed by co-migration with pure standards in HPLC. Strains produced 1,124 µg/ml of PCA, 2,700-14,200 µg/ml of PRN, 3,045-9,400 µg/ml of PLT and 2.5-930 µg/ml of DAPG. Production of antibiotics by strains was also confirmed by TLC analysis. The retardation factor (Rf) values were 0.77 for DAPG, 0.53 for PCA, 0.80 for PRN, 0.50 for PLT as determined by co-migration with pure standards.

Combined phylogenetic tree analysis based on *gyrB* and *rpoD* genes

Phylogenetic tree was constructed by combined data sets of *gyrB* and *rpoD*, assuming that the analysis using longer sequences would result in a better resolution and reliability. Phylogenetic analysis of antagonistic fluorescent pseudomonad strains resulted into 4 major clusters (Fig. 2). Cluster I consisted of 14 strains of *P. fluorescens* (P2, P3, P5, P7-P9, P14, P16-P19, and P21-P23) along with the reference strains *P. fluorescens* (ATCC 12983, ATCC 17467, ATCC 17573, ATCC 17574), *P. marginalis* (NCPPB3210, NCPPB949), and *P. aureofaciens* (now considered as *P. chlororaphis*) (NCIMB9265). Cluster II consisted of 4 strains of *P. putida* (P12, P15, P24, and P25) and 1 strain of *P. plecoglossicida* (P20) along with the reference strains, *P. putida* (IFO14671, KF715, ATCC 33015, PB4). Cluster III consisted of 2 strains of *P. pseudoalcaligenes* (P1, P4) along with the reference strains *P. pseudoalcaligenes* (IAM12410) and *P. oleovorans* (IFO13583). Cluster IV contained 3 strains of *P. aeruginosa* (P10, P11, P13) along with the reference strains, *P. aeruginosa* (IFO3080, IFO12689, IFO3446) and *P. citronellolis* (NCIMB12783). The sequences of *S. maltophilia* were treated as the out group in the phylogenetic tree and *P. aeruginosa* branched of first from the phylogenetic tree then diverged from the rest. Due to the high evolutionary rate of protein coding sequences, *gyrB* and *rpoD*

Table 4. Solubilization of tricalcium phosphate by antagonistic fluorescent pseudomonad strains

Pseudomonas species (Strains)	Incubation (Days)									
	1		3		5		7		10	
	pH	P solubilized#	pH	P solubilized#	pH	P solubilized#	pH	P solubilized#	pH	P solubilized#
P. fluorescens										
P2	6.3	11.44 ± 1.11^{e}	5.9	37.89 ± 0.83^{g}	5.5	58.24 ± 0.82^{h}	5.0	80.32 ± 0.46^{j}	4.4	103.2 ± 0.80^{j}
P3	6.3	14.21 ± 1.76^{f}	6.0	43.83 ± 0.25^{h}	5.3	66.19 ± 1.08^{i}	4.8	90.33 ± 0.28^{k}	4.5	99.65 ± 0.58^{j}
P5	6.5	10.08 ± 0.95^{d}	5.9	38.82 ± 0.15^{gh}	5.3	66.57 ± 0.42^{i}	5.0	81.12 ± 0.84^{jk}	4.4	105.3 ± 0.49^{j}
P7	6.6	6.80 ± 0.93^{c}	6.2	29.45 ± 0.94^{f}	5.9	51.77 ± 0.27^{g}	5.6	75.68 ± 0.62^{ij}	5.3	90.52 ± 0.71^{i}
P9	6.6	6.99 ± 0.94^{c}	6.0	38.58 ± 0.42^{gh}	5.3	58.57 ± 0.72^{h}	4.9	80.42 ± 2.85^{j}	4.5	94.87 ± 1.51^{ij}
P14	6.5	9.05 ± 1.58^{d}	6.0	40.37 ± 0.44^{h}	5.7	57.31 ± 0.77^{h}	4.9	83.28 ± 0.42^{jk}	4.5	99.97 ± 1.33^{j}
P16	6.7	5.16 ± 0.42^{b}	6.3	18.79 ± 0.16^{c}	5.8	40.71 ± 0.24^{e}	5.4	66.00 ± 0.05^{gh}	5.1	74.63 ± 0.29^{fg}
P17	6.4	15.53 ± 1.34^{fg}	5.9	36.34 ± 1.05^{g}	5.4	59.72 ± 0.56^{hi}	5.1	76.25 ± 0.37^{ij}	4.8	89.91 ± 0.67^{i}
P23	6.4	8.65 ± 1.07^{d}	6.1	26.70 ± 0.19^{e}	5.7	49.50 ± 0.37^{g}	5.3	69.13 ± 1.13^{h}	4.9	80.93 ± 1.05^{gh}
P. aeruginosa										
P10	6.6	5.50 ± 0.09^{b}	6.2	25.42 ± 0.70^{e}	5.9	39.03 ± 0.10^{d}	5.5	49.27 ± 0.52^{dc}	5.3	61.97 ± 0.40^{d}
P11	6.6	5.08 ± 1.08^{b}	6.1	19.92 ± 0.53^{c}	5.9	30.31 ± 0.51^{c}	5.7	38.37 ± 0.23^{c}	5.5	45.91 ± 0.27^{bc}
P13	6.6	4.55 ± 0.95^{ab}	6.2	21.08 ± 0.69^{d}	5.9	34.93 ± 0.57^{cd}	5.6	47.91 ± 0.4^{d}	5.3	63.17 ± 0.45^{dc}
P. putida										
P12	6.5	5.25 ± 0.71^{b}	6.1	26.70 ± 0.53^{e}	5.8	44.21 ± 0.47^{f}	5.3	56.79 ± 0.31^{f}	5.0	74.32 ± 0.87^{f}
P15	6.7	4.89 ± 0.07^{b}	6.3	23.18 ± 0.80^{d}	5.9	42.95 ± 0.68^{ef}	5.4	57.75 ± 0.20^{f}	5.2	71.33 ± 1.00^{f}
P24	6.7	5.63 ± 0.69^{b}	6.2	23.28 ± 0.05^{d}	5.9	38.90 ± 0.08^{d}	5.6	52.06 ± 0.10^{e}	5.2	76.33 ± 0.70^{g}
P25	6.8	4.39 ± 0.68^{a}	6.3	24.67 ± 0.15^{e}	5.9	46.10 ± 0.11^{f}	5.3	61.84 ± 0.07^{fg}	5.0	74.08 ± 0.69^{f}

Mean values with in the column followed by different superscript letters are significantly different according to Duncan's multiple range test ($p<0.05$). Data represents the average of three replications.# Phosphate solubilized in µg/ml±SE

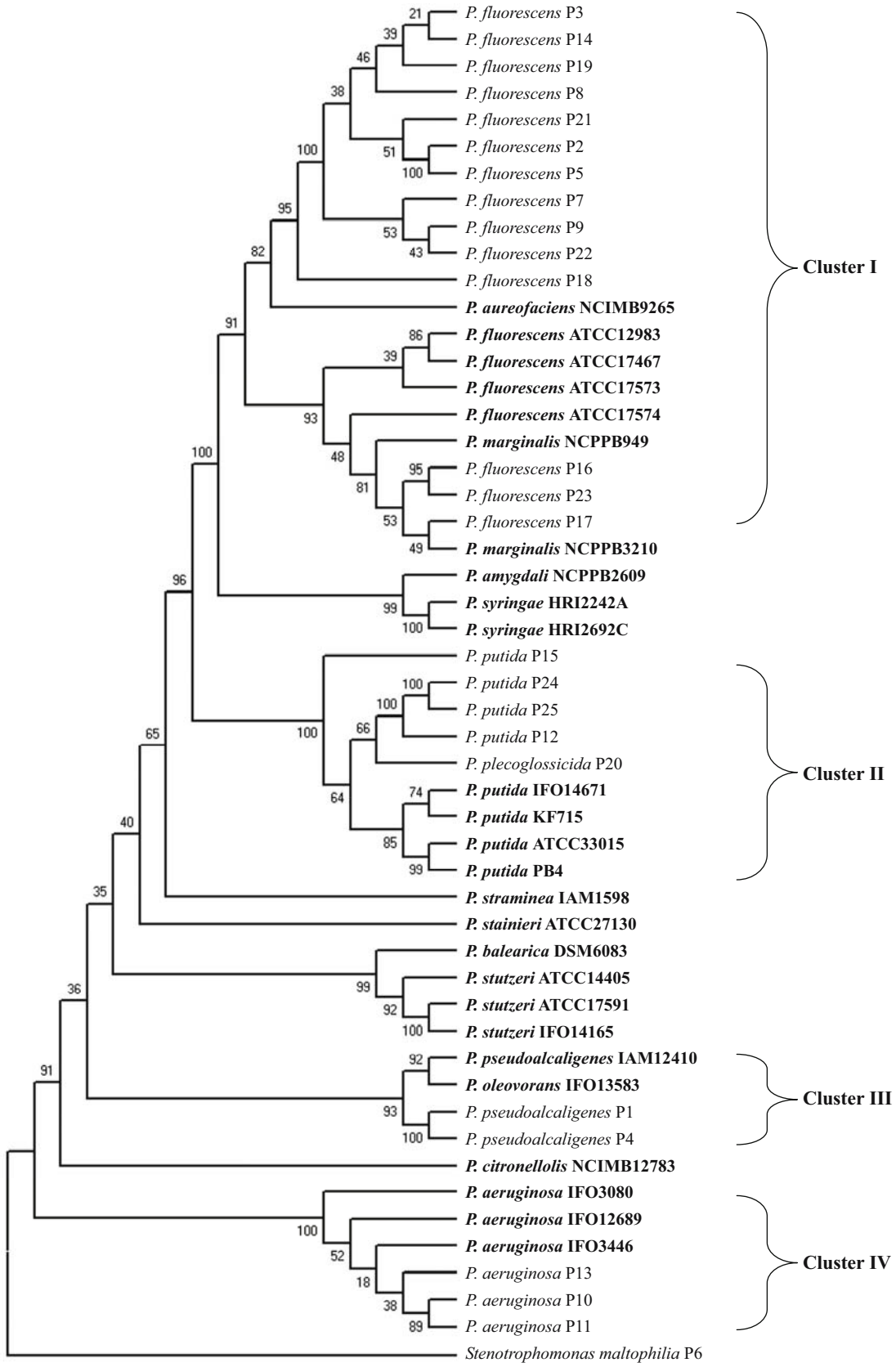

Fig. 2. Phylogenetic tree of antagonistic fluorescent pseudomonad strains based on the *gyrB* and *rpoD* sequences. The tree was constructed using neighbour-joining method. The sequences of *S. maltophilia* were treated as the out group.

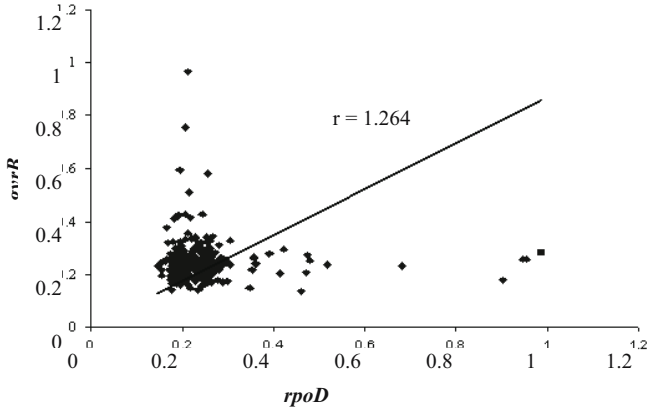

Fig. 3. Comparison between the genetic distances estimated from *gyrB* and *rpoD* genes of antagonistic fluorescent pseudomonad strains. The synonymous distances were obtained from nucleotide sequences of the *gyrB* and *rpoD* genes by applying the method of Nei and Gojobori (1986).

resulted into better resolution (Yamamoto *et al*., 2000).

Synonymous and non-synonymous genetic distance relationship of antagonistic fluorescent pseudomonads

Synonymous distances were obtained from nucleotide sequences of the *gyrB* and *rpoD* genes of antagonistic strains. Results revealed a good correlation between the synonymous distances (r value 1.2) among the *gyrB* and *rpoD* genes of antagonistic fluorescent pseudomonads (Fig. 3). These results explained the constant synonymous substitution rate among the antagonistic fluorescent pseudomonads. The number of synonymous substitutions per synonymous site (dS) and the number of non synonymous substitutions per non synonymous site (dN) for *gyrB* and *rpoD* sequences was also analyzed. We found that mostly dN is lower than dS (data not shown) which indicates the significant difference between sequence domains from species of the same genus. Results also substantiated that the genetic substitution rate in the protein coding sequences may be constant in antagonistic fluorescent pseudomonads.

ARDRA

The length (1,500 bp) of directly amplified PCR fragments of 16S rRNA from each strain was confirmed by standard agarose gel electrophoresis. Out of 11 restriction endonuclease enzymes (*Alu*I, *Bam*HI, *Pvu*II, *Hind*III, *Hae*III, *Hha*I, *Nhe*I, *Sph*I, *Pst*I, *Kpn*I, and *Taq*I) used, only *Alu*I, *Hae*III, and *Taq*I produced 3 to 6 distinct bands. ARDRA analysis differentiated the antagonistic strains belonging to the major groups of fluorescent pseudomonads such as *P. putida*, *P. fluorescens*, and *P. aeruginosa*. The similarity analysis showed the levels of genetic variation among the antagonistic fluorescent pseudomonads. The level of percentage similarity among the ARDRA ranged from 75 to 95% (data not shown). Strains were divided into two major groups and shared common routing at the similarity around 80%. Group I consisted of two clusters, which deviated from the common single nodal region. Cluster I was found to be a major and largest distinct group with 13 strains of *P. fluorescens* (P1-P5, P7, P9, P14, P17-P19, P21, and P22) with 82% similarity. On the other hand, cluster II consisted of 10 strains of (P6-P8, P10, P12, P15, P20, and P23-P25) *P. putida* and *P. fluorescens* along with other strains with 82% similarity value. The second group consisted of only two strains of *P. aeruginosa* (P11 and P13) with 80% similarity.

Genotypic analyses of antagonistic fluorescent pseudomonads

ARDRA analysis clearly classified the species within the groups of fluorescent pseudomonads strain but failed to show strain variations. Hence, attempts were made to differentiate strains using rep-PCR based whole genome fingerprinting analyses (ERIC, REP, and BOX PCR). ERIC-PCR analysis produced 18 genotypes, REP and BOX PCR produced 14 and 12 genotypes respectively (Table 5). However, individual rep-PCR based whole genome fingerprinting analyses also did not resolve the genetic variation among strains. Therefore, to improve the resolution of the analysis, the combined dendrogram was constructed based on the results of ERIC, REP, and BOX PCR. The rep-PCR analyses showed complex genomic fingerprints consisting of 4 to 12 amplified bands (3,000 to 100 bp) of varying intensity (Fig. 4). The combined rep-PCR analysis differentiated the strains belonging to the same species. Differences among the strains were assessed on the basis of banding pattern of the PCR products. Cluster analysis of combined rep-PCR genomic fingerprint patterns resulted into two major groups with approximately 70% similarity. Further, these two major groups are subdivided into six clusters (Fig. 4). Cluster I consisted of strains such as *P. fluorescens* P2, P16, P14, and *S. maltophilia* P6 shared approximately 35% similarity. Cluster II and III, the major clusters comprised five strains with maximum 32% similarity index. Interestingly, cluster II consisted of group of fluorescent pseudomonad strains such as *P. fluorescens* P3, P9, P22, *P. putida* P12, and *P. aeruginosa* P13 with approximately 10% similarity. On the other hand, cluster III consisted of *P. fluorescens* strains such as P5, P7, P8, P17 and P19 with the similarity index of approximately 30%. Cluster IV contained *P. aeruginosa* P10, P11, *P. putida* P24. Similarly, *P. fluorescens* P18, P21, and *P. putida* P25 and *P. plecoglossicida* P20 showed around 30% similarity index in the cluster V. Cluster VI contained *P. pseudoalcaligenes* P1 and P4, *P. putida* P15 and *P. fluorescens* P23 with 35% similarity index. *S. maltophila* P6 formed an out group. Rep-PCR based DNA fingerprinting analysis clearly differentiated the antagonistic fluorescent pseudomonads belonging to species of *P. fluorescens*, *P. putida*, *P. aeruginosa* and *P. pseudoalcaligenes*. Fingerprint profiles by rep-PCR clearly differentiated the species *P. fluorescens*. Though, these strains shared high level of similarity they varied in their DNA fingerprint patterns. Similarly, the *P. putida* strains P24 and P25 shared high degree of similarity but showed variable banding profiles. Minor variations were observed within the strains of *P. fluorescens* and *P. putida* as well as in the strains of *P. aeruginosa* and *P. pseudoalcaligenes*. All these results confirmed the genotypic diversity among antagonistic fluorescent pseudomonads.

Discussion

The present study described the genetic and functional relationship of antagonistic fluorescent pseudomonads associated in the rhizospheric soil of rice. The antagonistic strains were evaluated for their phenotypic diversity by culture-dependent analysis. It has been reported that, in comparison to other plant microenvironments, the rhizosphere is one of the main reservoirs of the antagonistic bacteria (Berg *et al*., 2005). Fluorescent pseudomonads have been reported as the predominant group of rhizosphere associated bacteria (Berg *et al*., 2006). The antagonistic bacteria reported in this study exhibited several beneficial traits such as production of IAA, phosphatase, and ACC deaminase. Earlier reports suggested that the strains possessing these beneficial traits can increase seed germination, plant growth and yield by competitive effects with the plant pathogens (Sakthivel and Gnanamanickam, 1987; Anjaiah *et al*., 2003; Bano and Mussarrat, 2003). Denitrifying character of the antagonistic bacteria may play major role in the rhizosphere competitiveness (Berg *et al*., 2002). Strains tested positive for PCA, PLT and PRN based on gene-specific PCR were further confirmed for their metabolite production by subsequent HPLC analysis. None of the tested strains produced all antibiotics simultaneously. It has been reported that some of the antibiotics in pseudomonads will not exist alone; especially PLT always coexists with other antibiotics such as DAPG or PRN (Raaijmakers *et al*., 1997). Although CFA is common to many fluorescent pseudomonads only antagonistic strains showed detectable amount of cyclopropane (17:0 CYCLO w7c). The CFA formation occurs primarily in the stationary phase of the growth cycle under the control of *rpoS* and indicated the overall efficiency of production of antibiotics controlled by the stationary phase regulators (Ellis *et al*., 2000).

The phenotypic traits were heterogeneous among the antagonistic fluorescent pseudomonads. Root exudates that contain amino acids, sugars, and organic acids are considered as important nutritional sources (Lottmann and Berg, 2001). Hence, the ability to utilize specific organic substrates may be considered as one of the important traits involved in the selection of antagonistic fluorescent pseudomonads and also as biological control agents. Utilization of the variety of carbon sources by fluorescent pseudomonads may play an important role in bacterial colonization (Anjaiah *et al*., 2003) and adaptation to a variety of crop plants and soil types. In our study, all functionally associated strains showed variable properties in utilization of carbon sources. To explore the potential genetic relationship, all the strains were analyzed by repetitive sequences and other phylogenetic and functional genes.

The protein coding sequences such as *gyrB* and *rpoD* reported in this study showed a better resolution in phylogeny.

Table 5. Genetic diversity of antagonistic fluorescent pseudomonads

Strain	Closest hits to sequences in NCBI database	rep-PCR			ARDRA			
		ERIC	REP	BOX	*Alu*I	*Hae*III	*Hha*I	*Taq*I
P1	*Pseudomonas pseudoalcaligenes*	E 1	R 1	BOX 1	A	A	A	A
P2	*Pseudomonas fluorescens*	E 2	R 2	BOX 2	A	A	A	B
P3	*Pseudomonas fluorescens*	E 2	R 2	BOX 2	B	A	A	B
P4	*Pseudomonas pseudoalcaligenes*	E 3	R 3	BOX 3	C	A	A	A
P5	*Pseudomonas fluorescens*	E 4	R 4	BOX 4	C	B	A	A
P6[a]	*Stenotrophomonas maltophilia*	E 5	R 5	BOX 5	C	A	B	A
P7	*Pseudomonas fluorescens*	E 3	R 6	BOX 4	C	A	A	A
P8	*Pseudomonas fluorescens*	E 4	R 5	BOX 4	C	A	A	A
P9	*Pseudomonas fluorescens*	E 6	R 7	BOX 6	C	A	A	B
P10	*Pseudomonas aeruginosa*	E 6	R 8	BOX 3	C	A	C	B
P11	*Pseudomonas aeruginosa*	E 7	R 7	BOX 6	D	A	C	A
P12	*Pseudomonas putida*	E 8	R 7	BOX 7	C	A	C	A
P13	*Pseudomonas aeruginosa*	E 9	R 9	BOX 3	C	C	C	A
P14	*Pseudomonas fluorescens*	E 10	R 10	BOX 8	C	C	D	A
P15	*Pseudomonas putida*	E 11	R 3	BOX 4	C	D	E	B
P16	*Pseudomonas fluorescens*	E 12	R 11	BOX 5	C	E	A	C
P17	*Pseudomonas fluorescens*	E 12	R 12	BOX 5	C	E	C	C
P18	*Pseudomonas fluorescens*	E 13	R 10	BOX 9	E	E	C	A
P19	*Pseudomonas fluorescens*	E 5	R 13	BOX 10	C	E	C	A
P20	*Pseudomonas plecoglossicida*	E 14	R 14	BOX 11	C	E	C	A
P21	*Pseudomonas fluorescens*	E 15	R 15	BOX 9	C	E	C	A
P22	*Pseudomonas fluorescens*	E 16	R 9	BOX 3	C	E	C	A
P23	*Pseudomonas fluorescens*	E 17	R 3	BOX 11	C	F	A	A
P24	*Pseudomonas putida*	E 18	R 14	BOX 12	C	E	C	A
P25	*Pseudomonas putida*	E 18	R 14	BOX 12	C	E	C	A

[a] Close relative of *Pseudomonas* group (formerly, *P. maltophilia*)

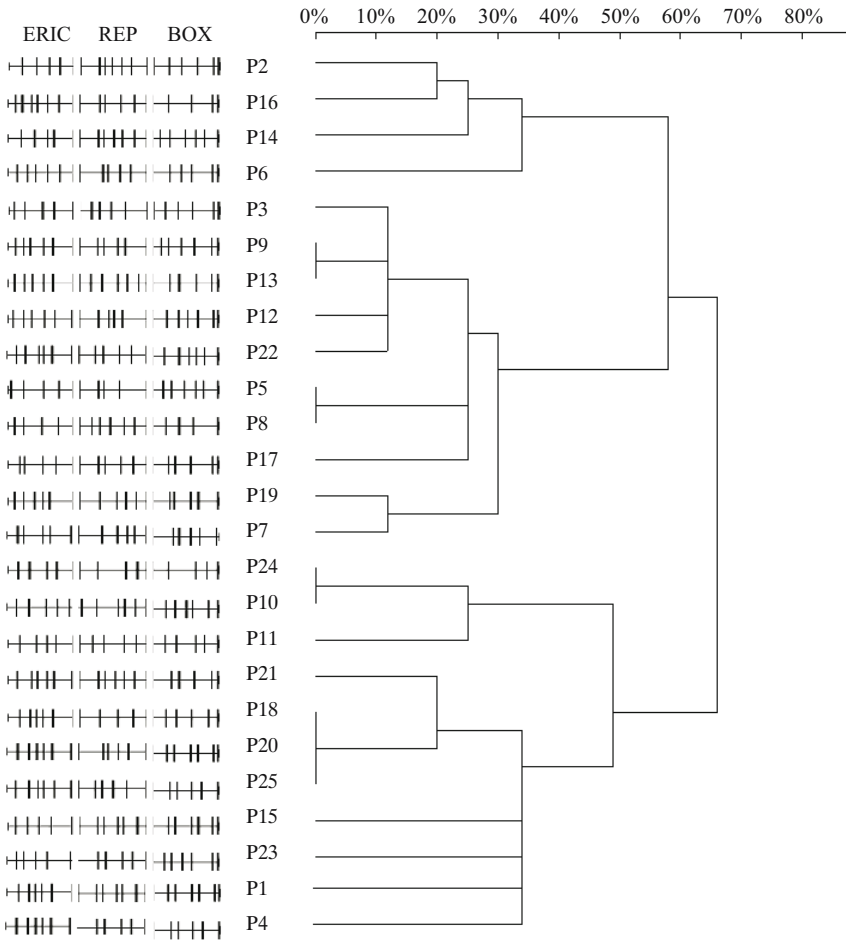

Fig. 4. Cluster analysis of combined (ERIC, REP, and BOX PCR) genomic fingerprint patterns of functionally associated fluorescent *Pseudomonas* of rice. The UPGMA algorithm was applied to the similarity matrix generated with Dice coefficient.

Molecular phylogeny deduced from a single locus may be unreliable due to the stochastic nature of base substitutions or to rare horizontal gene transfer events as suggested by Yamamoto and Harayama (1998); Yamamoto *et al*. (2000). The use of combined *gyrB* and *rpoD* sequences analysis would give a more accurate estimate of the phylogeny. This may be due to the high evolutionary rate of protein coding sequences, *gyrB* and *rpoD* (Yamamoto and Harayama, 1998; Yamamoto *et al*., 2000). Our analysis based on the combination of *gyrB* and *rpoD* sequences yielded a better resolution than 16S rRNA and also had a good agreement with previously reported FAME groups of fluorescent pseudomonads (Ayyadurai *et al*., 2007). Also, significant correlation between the genetic distances in the *gyrB* and *rpoD* genes has been obtained. These results suggested that the genetic substitution rate in the protein coding sequences is constant among the functionally associated fluorescent pseudomonads. Several functional genes such as *gacA*, *rpoB* and *oprF* were used for in-depth analysis of fluorescent pseudomonad diversity and evolutionary relationship (Costa *et al*., 2007). Our results on *gyrB* and *rpoD* sequence analysis reflect the evolutionary relatedness among antagonistic fluorescent pseudomonad strains. Also, there has been no previous report on the phylogenetic analysis of protein coding sequences from rice rhizosphere associated antagonistic bacteria.

ARDRA pattern by *Alu*I, *Hha*I, and *Taq*I allowed the clear discrimination of antagonistic fluorescent pseudomonads species such as *P. fluorescens*, *P. putida*, and *P. aeruginosa*. Depending on the restriction endonucleases used (*Alu*I, *Hha*I, and *Taq*I) 3 to 6 fragments were obtained. Strains produced a monomerphic ARDRA pattern when digested with other restriction enzymes. Enzyme *Hha*I generated pattern resulted into 6 ARDRA groups. However, DNA profile generated by restriction enzymes such as *Alu*I, and *Taq*I did not differentiate the antagonistic fluorescent pseudomonad strains. These ARDRA results confirmed the high levels of genetic heterogeneity among fluorescent pseudomonads as reported (Laguerre *et al*., 1994). The gene sequences encoding ribosomal DNA are strictly conserved and are nearly identical in almost all species and therefore, used for the differentiation of genera and species. Enzymes, used *Alu*I, *Hha*I, and *Taq*I produced specific patterns and facilitated grouping of subgroups of *P. fluorescens*, *P. aeruginosa*, and *P. putida* separately with distinct banding patterns but failed to differentiate among the strains belonging to the same subgroup.

Results of the rep-PCR analysis revealed the genomic

diversity among the fluorescent pseudomonad strains more precisely. However, rep-PCR based individual analysis of the DNA fingerprints was not sufficient to resolve their genetic variation. Therefore, to improve the genetic resolution a combined dendrogram was constructed based on the results of ERIC, REP and BOX PCR. Differences among the strains were assessed on the basis of the banding pattern of PCR products. The rep-PCR analysis clearly differentiated the functionally associated fluorescent pseudomonads. All these results revealed a better understanding on the genetic and functional relationship of the antagonistic fluorescent pseudomonads of rice rhizosphere. Current knowledge on the genetic structure of the antagonistic bacteria has practical importance since their utilization in agriculture requires evaluation of environmental risk, as well as an assessment of favorable microbial ecology. Successful biological control on the basis of plant rhizosphere associated antagonists not only requires a better knowledge of the complex regulation of disease suppression in response to biotic and abiotic factors, but also requires knowledge of the dynamics and composition of their community. CFA detection can be used as a marker for rapid screening of antagonistic strains. Data reported in this study by the polyphasic approach might be useful to understand the phylogenetic and functional potential of antagonistic fluorescent pseudomonads and to design biological control strategies for sustainable agriculture.

Acknowledgements

This work was supported by a grant from the Department of Biotechnology, Government of India, New Delhi. We thank J. M. Risede, UMR de pathologie Vegetale INRA-INH-Universite d'Angers, France for the supply of microbial cultures.

References

Anjaiah, V., P. Cornelis, and N. Koedam. 2003. Effect of genotype and root colonization in biological control of Fusarium wilts in pigeonpea and chickpea by *Pseudomonas aeruginosa* PNA1. *Can. J. Microbiol.* 49, 85-91.

Ayyadurai, N., P. Ravindra Naik, and N. Sakthivel. 2007. Functional characterization of antagonistic fluorescent pseudomonads associated with rhizospheric soil of rice (*Oryza sativa* L.). *J. Microbiol. Biotechnol.* 17, 919-927.

Ayyadurai, N., P. Ravindra Naik, M. Sreehari Rao, R. Sunish Kumar, S.K. Samrat, M. Manohar, and N. Sakthivel. 2006. Isolation and characterization of a novel banana rhizosphere bacterium as fungal antagonist and microbial adjuvant in micropropagation of banana. *J. Appl. Microbiol.* 100, 926-937.

Bano, N. and J. Mussarrat. 2003. Characterization of a new *Pseudomonas aeruginosa* strain NJ-15 as a potential biocontrol agent. *Curr. Microbiol.* 46, 324-328.

Berg, G., A. Krechel, M. Ditz, R. Sikora, A. Ulrich, and J. Hallmann. 2005. Endophytic and ectophytic potato-associated bacterial communities differ in structure and antagonistic function against plant pathogenic fungi. *FEMS Microbiol. Ecol.* 51, 215-229.

Berg, G., K. Opelt, C. Zachow, J. Lottmann, M. Gotz, R. Costa, and K. Smalla. 2006. The rhizosphere effect on bacterial antagonistic towards the pathogenic fungus *Verticillium* differs depending on plant species and site. *FEMS Microbiol. Ecol.* 56, 250-261.

Berg, G., N. Roskot, A. Steidle, L. Eberl, A. Zock, and K. Smalla. 2002. Plant-dependent genotypic and phenotypic diversity of antagonistic rhizobacteria isolated from different *Verticillium* host plants. *Appl. Environ. Microbiol*. 68, 3328-3338.

Bhattacharya, D., P.M. Sarma, S. Krishnan, S. Mishra, and B. Lal. 2003. Evaluation of genetic diversity among *Pseudomonas citronellolis* strains isolated from oily sludge-contaminated sites. *Appl. Environ. Microbiol.* 69, 1435-1441.

Bossis, E., P. Lemanceau, X. Latour, and L. Garden. 2000. The Taxonomy of *Pseudomonas fluorescens* and *Pseudomonas putida*: current status and need for revision. *Agronomie* 20, 51-63.

Bric, M., M. John, R. Bostock, and R.E. Silverstone. 1991. Rapid in situ assay for indoleacetic acid production by bacteria immobilized on a nitrocellulose membrane. *Appl. Environ. Microbiol.* 57, 535-538.

Brown, J.L., T. Brown, T.A. Ross, N. McMeekin, and P.D. Nichols. 1997. Acid habituation of *Escherichia coli* and the potential role of cyclopropane fatty acids in low pH tolerance. *Int. J. Food Microbiol.* 37, 163-173.

Cai, J.J., D.K. Smith, X. Xia, and K. Yuen. 2005. MBEToolbox: a Matlab toolbox for sequence data analysis in molecular biology and evolution. *BMC Bioinfor.* 6, 63-71.

Costa, R., N.C.M. Gomes, E. Krogerrecklenfort, K. Opelt, G. Berg, and K. Smalla. 2007. *Pseudomonas* community structure and antagonistic potential in the rhizosphere: insights gained by combining phylogenetic and functional gene-based analyses. *Environ. Microbiol.* 9, 2260-2273.

Delorme, S., L. Philippot, V. Edel-Hermann, C. Deulvot, C. Mougel, and P. Lemanceau. 2003. Comparative genetic diversity of the *narG*, *nosZ*, and 16S rRNA genes in fluorescent pseudomonads. *Appl. Environ. Microbiol.* 69, 1004-1012.

de Souza, J.T. and J. M. Raaijmakers. 2003. Polymorphisms within the *PrnD* and *PltC* genes from pyrrolnitrin and pyoluteorin-producing *Pseudomonas* and *Burkholderia* spp. *FEMS Microbiol. Ecol.* 43, 21-34.

Dye, D.W. 1962. The inadequacy of the usual determinative tests for identification of *Xanthomonas* spp. *Newzealand J. Sci*. 5, 393-416.

Ellis, R.J., T.M. Timms Wilson, and M.J. Bailey. 2000. Identification of conserved traits in fluorescent pseudomonads with antifungal activity. *Environ. Microbiol.* 2, 274-284.

Emmert, E.A.B. and J. Handelsman. 1999. Biocontrol of plant disease: A (Gram) positive perspective. *FEMS Microbiol. Lett.* 171, 1-9.

Gorden, S.A. and R.P. Weber. 1951. Colorimetric estimation of indoleacetic acid. *Plant Physiol*. 26, 192-195.

Grogan, D.W. and J.E. Cronan. 1997. Cyclopropane ring formation in membrane lipids of bacteria. *Microbiol. Mol. Biol. Rev.* 61, 429-441.

Higgins, D.G., A.T. Bleashy, and R. Fuchs. 1992. Clustal V: Improved software for multiple sequence alignment. *Comput. Appl. Biosci.* 8, 189-191.

Keel, C., U. Schnider, M. Maurhofer, C. Voisard, M. Burger, P. Wirthner, D. Haas, and G. Defago. 1992. Suppression of root disease by *Pseudomonas fluorescens* CHAO: importance of bacterial secondary metabolite 2,4-diacetylphloroglucinol. *Mol. Plant. Microbe Interact.* 5, 4-13.

Kimura, M. 1980. A simple method for estimating evolutionary rates of base substitutions through comparative studies of nucleotide sequences. *J. Mol. Evol.* 16, 111-120.

King, J.E. 1936. The colorimetric determination of phosphorus. *Biochem. J*. 26, 292-297.

King, E.O., M.K. Ward, and D.E. Raney. 1954. Two simple media for demonstration of pyocyanin and fluorescein. *J. Lab. Clin. Med.* 44, 301-307.

Kumar, B.S.D. and H.S. Dube. 1992. Seed bacterization with a fluorescent *Pseudomonas* for enhanced plant growth, yield and disease control. *Soil Biol. Biochem.* 24, 539-542.

Kumar, S., K. Tamura, I.B. Jakobsen, and M. Nei. 2001. MEGA2: molecular evolutionary genetics analysis software. *Bioinfor*. 17,

1244-1245.

Laguerre, G., L. Rigottier-Gois, and P. Lemanceau. 1994. Fluorescent *Pseudomonas* species categorized by using polymerase chain reaction (PCR) / restriction fragment analysis of 16S rDNA. *Mol. Ecol.* 3, 479-487.

Leach, J.E., M.L. Rhoades, C.M.V. Cruz, F.F. White, T.W. Mew, and H. Leung. 1992. Assessment of genetic diversity and population structure of *Xanthomonas oryzae* with a repetitive DNA element. *Appl. Environ. Microbiol.* 58, 2188-2195.

Lottmann, J. and G. Berg. 2001. Phenotypic and genotypic characterization of antagonistic bacteria associated with roots of transgenic and non transgenic potato plants. *Microbiol. Res.* 156, 75-82.

Nei, M. and T. Gojobori. 1986. Simple methods for estimating the numbers of synonymous and nonsynonymous nucleotide substitutions. *Mol. Biol. Evol.* 3, 418-426.

Patten, C.L. and B.R. Glick. 2002. Role of *Pseudomonas putida* indoleacetic acid in development of the host plant root system. *Appl. Environ. Microbiol*. 68, 3795-3801.

Penrose, D.M. and B.R. Glick. 2002. Methods for isolating and characterizing ACC deaminase containing plant growth promoting rhizobacteria. *Physiol. Plantarum.* 118, 10-15.

Raaijmakers, J., D.M. Weller, and L.S. Thomashow. 1997. Frequency of antibiotic producing *Pseudomonas* spp. in natural environments. *Appl. Environ. Microbiol.* 63, 881-887.

Rainey, P.B. and E.R. Moxon. 2000. When being hyper keeps you fit. *Science* 288, 1186-1187.

Rangarajan, S., P. Loganathan, L.M. Saleena, and S. Nair. 2001. Diversity of pseudomonads isolated from three different plant rhizospheres. *J. Appl. Microbiol.* 91, 742-749.

Ravindra, N.P., N. Sahoo, D. Goswami, N. Ayyadurai, and N. Sakthivel. 2008. Genetic and functional diversity among fluorescent pseudomonads isolated from the rhizosphere of banana. *Microb. Ecol.* 56, 492-504.

Ravindra, N.P. and N. Sakthivel. 2006. Functional characterization of a novel hydrocarbonoclastic *Pseudomonas* sp. strain PUP6 with plant-growth-promoting traits and antifungal potential. *Res. Microbiol.* 157, 538-546.

Saitou, N. and M. Nei. 1987. The neighbor-joining method: a new method for reconstructing phylogenetic trees. *Mol. Biol. Evol.* 4, 406-425.

Sakthivel, N. and S.S. Gnanamanickam. 1987. Evaluation of *Pseudomonas fluorescens* for suppression of sheath rot disease and for enhancement of grain yields in rice (*Oryza sativa* L.). *Appl. Environ. Microbiol.* 53, 2056-2059.

Schwyn, B. and J.B. Neiland. 1987. Universal chemical assay for the detection and determination of siderophores. *Analy. Biochem*. 160, 47-56.

Sharp, P.M. 1997. In search of molecular darwinism. *Nature* 385, 111-112.

Sunish, K.R., N. Ayyadurai, P. Pandiaraja, A.V. Reddy, Y. Venkateshwarlu, O. Prakash, and N. Sakthivel. 2005. Characterization of antifungal metabolite produced by a new strain *Pseudomonas aeruginosa* PuPa3 that exhibits broad-spectrum antifungal activity and biofertility traits. *J. Appl. Microbiol.* 98, 145-154.

Thomashow, L.S., D.M. Weller, R.F. Bonsall, and L.S. Pierson. 1990. Production of the antibiotic phenazine-1-carboxylic acid of fluorescent *Pseudomonas* species in the rhizosphere of wheat. *Appl. Environ. Microbiol.* 56, 908-912.

Weisburg, W.G., S.M. Barns, and D.J. Lane. 1991. 16S ribosomal DNA amplification for phylogenetic study. *J. Bacteriol.* 173, 697-703.

Yamamoto, S. and S. Harayama. 1998. Phylogenetic relationships of *Pseudomonas putida* strains deduced from the nucleotide sequences of *gyrB*, *rpoD* and 16S rRNA genes. *Int. J. Syst. Bacteriol.* 48, 813-819.

Yamamoto, S., H. Kasai, D.L. Arnold, R.W. Jackson, A. Vivian, and S. Harayama. 2000. Phylogeny of the genus *Pseudomonas*: intrageneric structure reconstructed from the nucleotide sequences of *gyrB* and *rpoD* genes. *Microbiology* 146, 2385-2394.